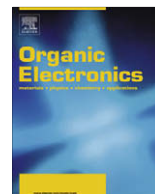




Contents lists available at ScienceDirect

## Organic Electronics

journal homepage: [www.elsevier.com/locate/orgel](http://www.elsevier.com/locate/orgel)

## Solution-processed single walled carbon nanotube electrodes for organic thin-film transistors

Adrian Southard<sup>a,b</sup>, Vinod Sangwan<sup>a,b,c</sup>, Jeremy Cheng<sup>a,b,c</sup>, Ellen D. Williams<sup>a,b,c</sup>, Michael S. Fuhrer<sup>a,b,\*</sup><sup>a</sup> Department of Physics, University of Maryland, College Park, MD 20742, USA<sup>b</sup> Center for Nanophysics and Advanced Materials, University of Maryland, College Park, MD 20742, USA<sup>c</sup> Laboratory for Physical Sciences, University of Maryland, College Park, MD 20742, USA

## ARTICLE INFO

## Article history:

Received 23 March 2009

Received in revised form 7 August 2009

Accepted 1 September 2009

Available online xxx

## PACS:

72.80.Le

73.40.Cg

73.61.Ph

73.63.Fg

## Keywords:

Organic thin-film transistor

Carbon nanotube

Pentacene

Poly-3-hexylthiophene

Contact resistance

Transparent electrode

## ABSTRACT

Airbrushed single walled carbon nanotube (SWCNT) thin films with sheet resistivity  $<1 \text{ k}\Omega/\text{sq}$ . and transparency  $>80\%$  are used as electrodes for pentacene and regioregular poly(3-hexylthiophene) (P3HT) thin-film transistors (TFTs). Airbrushed SWCNT electrodes show low contact resistance in a bottom-contact configuration, comparable to (in the case of P3HT) or lower than (in the case of pentacene) Au bottom-contacts. The results show that airbrushed CNT electrodes yield similar performance to CVD-grown CNT electrodes.

© 2009 Published by Elsevier B.V.

### 1. Introduction

Research in flexible, transparent organic electronics has been motivated by a wide range of applications [1,2] such as flexible “electronic paper” displays [3,4], radio frequency identification tags [5], photosensors [6], and solar cells [7]. However, the challenge lies in finding inexpensive, robust techniques for processing flexible, transparent electronics [2]. Currently oxide semiconductors (e.g. indium tin oxide or ITO) are widely used as transparent, conducting films in organic electronics applications. These materials are inher-

ently brittle, and require relatively expensive vacuum deposition techniques. Individual single walled carbon nanotubes (SWCNTs) are transparent in the visible and IR due to their high aspect ratio, show conductivity comparable to copper [8], and are environmentally stable [9]. SWCNT films have high mechanical flexibility, conductivity and transparency approaching that of ITO [9], and can be prepared inexpensively without vacuum equipment through solution techniques such as microfiltration [4,10], airbrushing [11–13], dipcoating [12,14], and electrophoretic deposition [15].

Understanding the electrical properties and limitations of the SWCNT/organic semiconductor interface is important to fully realize applications of transparent, conducting SWCNT films such as organic light-emitting diodes [3,4,16] and solar cells [17]. Previous work using SWCNT films

\* Corresponding author. Address: Department of Physics, University of Maryland, College Park, MD 20742, USA. Tel.: +1 301 405 0801.

E-mail address: [mfuhrer@umd.edu](mailto:mfuhrer@umd.edu) (M.S. Fuhrer).

grown by chemical vapor deposition (CVD) found a SWCNT/pentacene contact resistance as low as 30 k $\Omega$  cm ( $V_G = -50$  V) [18]. However, the CVD method is expensive and laborious, so solution-phase preparation of CNT films is more desirable for applications. Solution-processed CNTs have also been found to make good contact to poly(3,3'-didodecylquaterthiophene) [19], but it is not clear that this result could be expanded to pentacene, where contact resistance in bottom-contacted devices is more problematic. Here, we demonstrate transparent films of commercially-available SWCNTs produced by airbrushing from aqueous solution as electrodes for pentacene and poly-3-hexylthiophene (P3HT) thin-film transistors (TFTs). Airbrushing CNT thin films is an additive process that allows quick, large area patterning over any substrate and is compatible with ink-jet printing. CNT films deposited by spraying have been found to be rougher but exhibit similar sheet resistance for a given transparency as most other methods [14]. The channel-length-dependent output characteristics of the SWCNT-contacted TFTs on SiO<sub>2</sub>/Si substrates are used to extract the mobility  $\mu$  (0.093 cm<sup>2</sup>/Vs for pentacene, 0.014 cm<sup>2</sup>/Vs for P3HT) and contact resistivity. In the case of pentacene, we demonstrate that solution-processed SWCNT bottom-contact electrodes make moderately low-resistance (as low as 30 k $\Omega$  cm) contacts, which extends previous results for pentacene contacted by CVD-grown SWCNTs [20] to this much more easily processed material. For P3HT, we verify low contact resistance (<50 k $\Omega$  cm) bottom-contact to solution-processed SWCNTs, similar to previous results for poly(3,3'-didodecylquaterthiophene) [19]. We also demonstrate the use of solution-processed films of SWCNTs as source, drain, and gate electrodes to fabricate flexible, transparent SWCNT-contacted pentacene TFTs on plastic polyethylene terephthalate (PET) substrates.

## 2. Materials and methods

SWCNT films were prepared as follows. A dispersion of 1 mg/mL SWCNTs ("P3", carbon solutions) in 1% by wt. sodium dodecyl sulfate (SDS) and water was exfoliated by sonication for 90 min followed by differential centrifugation at 12,000 rpm for one hour to remove carbonaceous impurities [4]. The top 2/3 of the supernatant was extracted and used as the airbrush feedstock. The source/drain (S/D) electrodes of the test devices were made by using an airbrush (Aztek A470 airbrush kit) to deposit a 30–40 nm thick film onto a 500 nm-SiO<sub>2</sub>/n<sup>++</sup>-Si platform at a temperature of 165 °C. The deposited films are then soaked in water for one hour to remove surfactant, and dried with a N<sub>2</sub> gun. The SWCNT film was patterned using photolithography and O<sub>2</sub> reactive ion etching. In order to determine the organic-SWCNT contact resistance, a set of devices of varying gate length  $L$  from 3 to 1262  $\mu$ m was fabricated; the channel width  $W$  is 1.6–2.0 mm. The optical transparency of the carbon nanotube thin-film  $T$  was obtained from the ratio of the measured transparency of CNT-coated PET, prepared by airbrushing directly onto PET, to that of the PET substrate prior to nanotube coating.

Pentacene films were deposited onto the prepared electrodes in vacuum (<2  $\times$  10<sup>-7</sup> torr) by evaporation through

a shadow mask to form the active area of the TFT. P3HT transistors were fabricated on the prepared electrodes by first vapor coating the SiO<sub>2</sub> substrate with hexamethyldisilazane and then spin casting P3HT at 1250–2000 rpm from trichlorobenzene heated to 100 °C at a concentration of 10 mg/mL followed by a vacuum bake at 100 °C for one hour [21]. The doped Si substrate acts as a back-gate electrode. All electrical characterization was done in a N<sub>2</sub> atmosphere in the dark to prevent unintentional doping during the measurements.

## 3. Results and discussion

### 3.1. Carbon nanotube thin films as transparent electrodes

Fig. 1 shows the optical transparency  $T$  of the airbrushed CNT films as a function of film sheet resistance. The airbrushed films have a sheet resistance as low as 1 k $\Omega$ /sq. for  $T = 80\%$ , and 5 k $\Omega$ /sq. for  $T = 90\%$ , compared with 0.0278 k $\Omega$ /sq. @ 80% $T$  for ITO coated glass [22]. The method of dispersing SWCNTs and subsequently spraying them to form a thin-film has been reported by several groups [12–14]. The  $T$  vs. sheet resistance behavior is in agreement with a model proposed by Hu et al. [23] which predicts.

$$\%T = \frac{100}{\left(1 + \frac{2\pi}{cR_{\square}} \frac{\sigma_{ac}}{\sigma_{dc}}\right)^2} \quad (1)$$

where  $R_{\square}$  is the sheet resistance,  $\sigma_{ac}$  is the optical conductivity,  $\sigma_{dc}$  is the dc conductivity, and  $c$  is the speed of light; a fit to Eq. (1) is shown in Fig. 1. The only free parameter used is the ratio of  $\sigma_{ac}$  to  $\sigma_{dc}$ ; we find that a ratio of 0.74  $\pm$  0.03 gives the best fit to the data. This value is slightly smaller than the value of 1 obtained by Hu et al. [23].

### 3.2. Pentacene and P3HT transistors with carbon nanotube electrodes

Scanning electron microscopy was performed on the pentacene/SWCNT TFTs after electrical measurement of

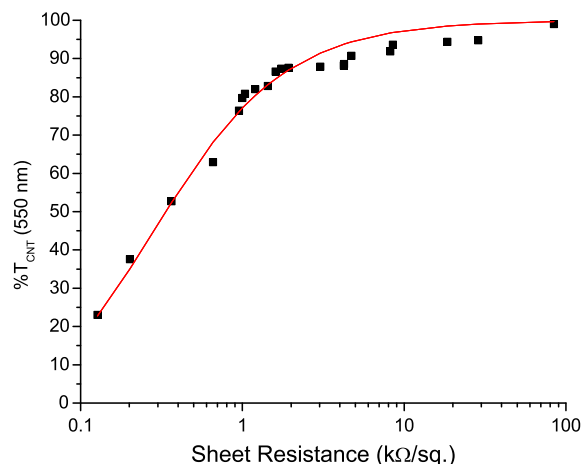


Fig. 1. The percent transparency at a wavelength of 550 nm vs. sheet resistance of airbrushed carbon nanotube films and fit using Eq. (1).

the transistors. Parts of one of the pentacene/SWCNT TFT are shown in Fig. 2a and Fig. 2b (a closeup) illustrating the morphology of the pentacene layer on both the bare SiO<sub>2</sub> as well as the CNT film. The pentacene on the bare SiO<sub>2</sub> forms ~250 nm grains separated by relatively thin grain boundaries whereas the pentacene on the CNT film forms a discontinuous film of rod-like grains. The crystal structure of these grains is unknown at this time and is the subject of further investigation.

Fig. 3a and b show output characteristics for example pentacene/SWCNT and P3HT/SWCNT TFTs, respectively. The resistance  $R$  of each device was found as a function of  $L$  and gate voltage  $V_G$  from the slope of drain current vs. drain voltage  $I(V_D)$  for  $-1 \text{ V} < V_D < 1 \text{ V}$ . A threshold voltage  $V_T$  was extracted from the conductance vs.  $V_G$  plot for each channel length; this allowed us to compare measurements performed at the same effective gate voltage  $V_G^* = V_G - V_T$ , correcting for any possible length-dependent threshold shift [24].

Fig. 4a and b show  $R$  vs.  $L$  at various values of  $V_G^*$  for the pentacene/SWCNT and P3HT/SWCNT TFTs respectively.  $R$  vs.  $L$  obeys a linear relationship  $R(L, V_G^*) = \alpha(V_G^*)L + R_c(V_G^*)$ . The intrinsic field-effect mobility may be found from  $\alpha$  [25]:

$$\mu_{FE}(V_G^*) = \frac{1}{WC_{ox}} \frac{\partial(\alpha^{-1})}{\partial V_G^*}. \quad (2)$$

The contact resistivity is defined to be  $\rho_c = R_c W$ , where  $W$  is the channel width. For pentacene/SWCNT devices,  $\rho_c$  is finite and gate voltage dependent, saturating at  $<30 \text{ k}\Omega \text{ cm}$  for  $V_G^* < -40 \text{ V}$ . Values for the contact resistance using Au bottom-contacts vary from 20 to 110 k $\Omega \text{ cm}$  depending on the gate voltage applied, the work function and conductivity of the injecting electrode, the temperature of the substrate during deposition and the thickness of the pentacene layer [26,27]. Au top contacts exhibit contact resistances an order of magnitude smaller [27]. In our devices, the intrinsic mobility is  $0.093 \text{ cm}^2/\text{Vs}$ . On/off current ratios ( $V_D = -60 \text{ V}$ ,  $-60 \text{ V} \leq V_G \leq 60 \text{ V}$ ) were  $>10^6$ . For P3HT/SWCNT devices,  $\rho_c$  is less than  $50 \text{ k}\Omega \text{ cm}$  at all gate voltages in the ON state, higher than control devices fabricated with Au bottom-

contacts whose  $\rho_c$  is  $1\text{--}10 \text{ k}\Omega \text{ cm}$  [25,28]. Intrinsic field-effect mobility was as high as  $0.014 \text{ cm}^2/\text{Vs}$ . On/Off current ratios  $>10^5$  ( $V_D = -60 \text{ V}$ ,  $-60 \text{ V} \leq V_G \leq 50 \text{ V}$ ) were obtained for P3HT/SWCNT devices.

The bottom-contact resistance obtained with Au deposited on a relatively thin Cr or Ti wetting layer as is typically used to make bottom-contacts is higher than that for Au top contacts, and shows non-linear  $I(V_D)$  characteristics, attributed to the presence of an injection barrier [29] or disruption of the pentacene morphology at the interface of the bottom-contacts [30]. Thus our observation that bottom-contact SWCNT electrodes offer slightly lower contact resistance to pentacene might either be due to narrowing of the injection barrier due to the high electric field at the SWCNT ends [31], or by allowing better ordering of the pentacene on SiO<sub>2</sub> at the electrode interface. Given the close packing of SWCNTs in our thick (30–40 nm) SWCNT film, and the thick (500 nm) gate dielectric, we consider electric-field enhancement unlikely. We propose that SWCNT electrodes allow more favorable growth of pentacene on the neighboring SiO<sub>2</sub> substrate, or that the morphology of pentacene on the SWCNTs themselves does not give rise to a significant injection barrier. In the case of P3HT, SWCNT contacts show a contact resistance similar to that obtained with Au [25,32,33].

### 3.3. Demonstration of transparent organic thin-film transistors

Finally, we show that solution-processed SWCNT electrodes can be used to fabricate an all-carbon transparent, flexible TFT in which SWCNT films are used as the source, drain, and gate electrodes, and pentacene as the semiconductor. Cao et al. demonstrated a SWCNT-contacted pentacene thin-film transistor (TFT) on a plastic substrate using SWCNTs grown by chemical vapor deposition (CVD) and patterned by photolithography [33]. Here, SWCNT gate electrodes were airbrushed through a shadow mask onto PET (Dupont Teijin™ Melinex 454/700; thickness  $170 \sim \mu\text{m}$ ). The SWCNT gate had a sheet resistance of  $3.1 \text{ k}\Omega/\text{sq}$  and a transparency of  $>91\%$  that was interpolated from the sheet resistance vs. transparency fit using Eq. (1).

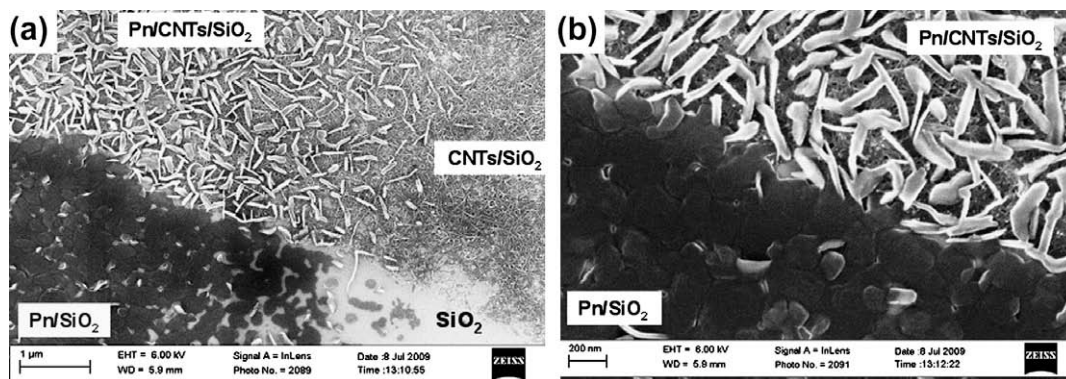
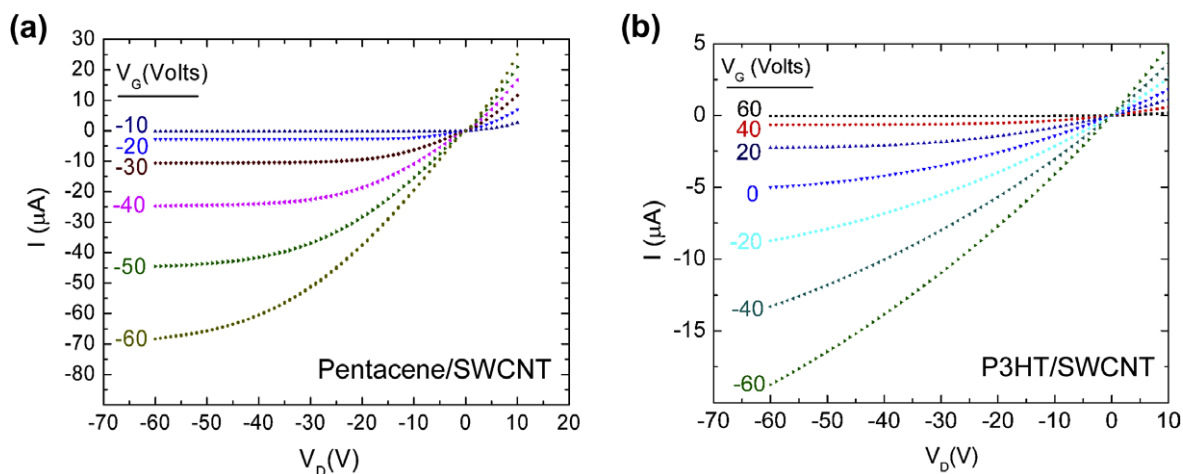
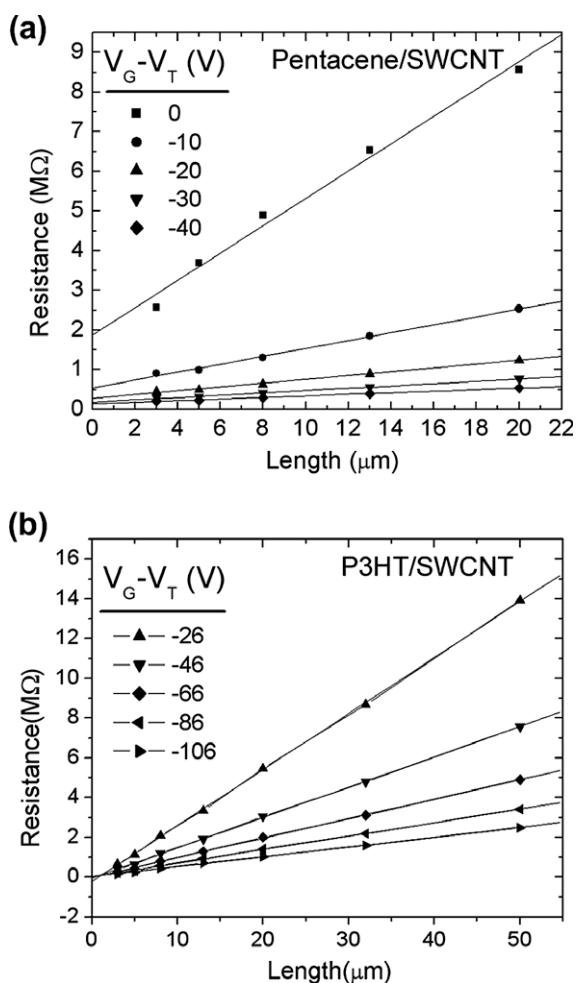


Fig. 2. Scanning electron micrographs of parts of one of the CNT/pentacene transistors showing (a) four separate areas: the bare SiO<sub>2</sub> (bottom right), the CNT film deposited on SiO<sub>2</sub> (upper right), the pentacene layer deposited on the same CNT film (upper left), the pentacene layer deposited on SiO<sub>2</sub> (bottom left) and (b) a closeup of the interface between the pentacene on SiO<sub>2</sub> and the pentacene on the CNT film.



**Fig. 3.** (a) Output characteristics of a carbon nanotube film-contacted pentacene transistor with length  $L = 20 \mu\text{m}$ , width  $W = 1600 \mu\text{m}$ . (b) Output characteristics of a poly-3-hexylthiophene thin-film transistor with carbon nanotubes electrodes with length  $L = 50 \mu\text{m}$ , width  $W = 2000 \mu\text{m}$ .



**Fig. 4.** (a) Resistance vs. channel length for effective gate voltages  $V_G - V_T = 0-60 \text{ V}$  in  $10 \text{ V}$  steps for carbon nanotube film-contacted pentacene transistors and (b) carbon nanotubes film-contacted P3HT transistors with  $V_G - V_T = -26$  to  $-106$  in  $20 \text{ V}$  steps.

To facilitate probing the CNT layer, a  $100 \text{ nm}$  Au layer was deposited onto the four sides of the CNT gate electrode. The dielectric layer was applied in two steps. In the first step, a  $1 \mu\text{m}$  thick layer of PMMA was spun cast onto a transfer substrate and printed onto the device substrate at  $500 \text{ psi}$  and  $T = 170 \text{ }^\circ\text{C}$  for three minutes [34]. In the second step, SWCNT source and drain electrodes (sheet resistance of  $1 \text{ k}\Omega/\text{sq}$  and  $T > 78\%$ ) were patterned on a  $\text{SiO}_2/\text{Si}$  transfer substrate following the scheme outlined above, coated with  $50 \text{ nm}$  of alumina (electron beam evaporation at  $2 \times 10^{-6} \text{ torr}$ ) followed by a  $1 \mu\text{m}$  thick spin coated layer of PMMA and then printed onto the device substrate. The alumina layer served to minimize the leakage current from the source and drain electrodes to the gate. The capacitance of the resulting gate dielectric is estimated to be  $1.33 \text{ nF}/\text{cm}^2$ . Finally,  $30 \text{ nm}$  thick pentacene was evaporated through a shadow mask as described earlier to complete the devices. Devices had a channel width of  $97-98 \mu\text{m}$  and channel length from  $37$  to  $47 \mu\text{m}$ .

Fig. 5a shows a micrograph of the completed device. The single cross-shaped CNT film acts as a common gate for all four transistors. Silver paint was applied to the ends of two of the gate contacts to facilitate repeated probing of the CNT film. Fig. 5b shows the output characteristics of the device. The field-effect mobility obtained for these devices (uncorrected for contact resistance) was as high as  $0.06 \text{ cm}^2/\text{Vs}$  with an average of  $0.04 \text{ cm}^2/\text{Vs}$ , assuming a dielectric constant for PMMA of  $3.6$ . As fabricated, the devices exhibited  $V_T > 60 \text{ V}$ , so the on/off current ratio could not be accurately determined. After aging the devices for several months in an inert environment ( $< 0.1 \text{ ppm}$  moisture content) the threshold voltages shifted to between  $-10$  and  $-20 \text{ V}$  indicating diffusion of dopants out of the device over time. The on/off current ratios for the aged devices ranged from  $10^3$  to  $10^4$  ( $V_D = -60 \text{ V}$ ,  $-60 \text{ V} \leq V_G \leq 60 \text{ V}$ ), and the saturation mobility values decreased by  $10-15\%$ . The low on/off current ratios compared to devices on  $\text{SiO}_2$  are likely due to the more than four times lower gate capacitance as well as possibly charge trapping at

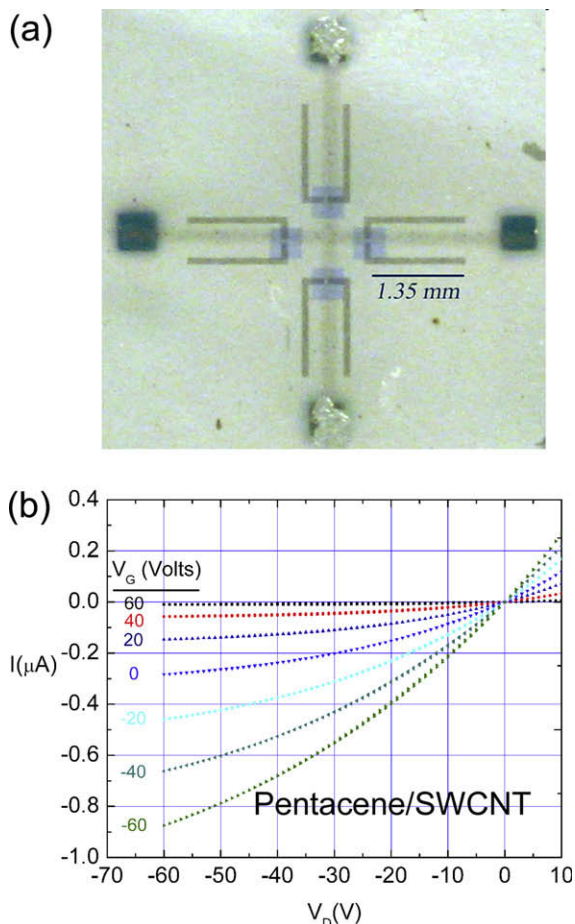


**Fig. 5.** (a) Optical micrograph of four transparent, flexible carbon nanotube film-contacted pentacene thin-film transistors (TFTs) on polyethylene terephthalate (PET) substrate. (b) Output characteristics for one of the TFTs pictured in (a).

the pentacene/ $\text{Al}_2\text{O}_3$  interface which prevent the off state from being reached.

#### 4. Conclusion

In conclusion, we have used airbrushed SWCNT films with sheet resistance below  $1 \text{ k}\Omega/\text{sq}$  at  $T = 80\%$  as electrodes to make bottom-contact pentacene transistors with contact resistance as low as  $26 \text{ k}\Omega \text{ cm}$ , lower than typically achievable with Au/Cr bottom-electrodes, and comparable to results achievable with CVD-grown CNTs. If we assume that the organic/CNT contact resistance is inversely proportional to mobility [25] even lower contact resistance should be possible with organic films optimized for higher mobility. The low contact resistance between the pentacene and CNT film is surprising given the significant differences in morphology observed for pentacene deposited on  $\text{SiO}_2$  vs. CNTs (see Fig. 2). Solution-processed SWCNT films also make bottom-contact electrodes to P3HT with contact resistance comparable to that of Au. We have also demon-

strated that solution-processed electrodes can be patterned onto a flexible plastic substrate both directly (gate electrode with transparency  $>91\%$ ) and via transfer printing (source-drain electrode), as components of a Pn TFT (with  $>78\%$  transparency) using a relatively transparent PMMA/ $\text{Al}_2\text{O}_3$  dielectric and PET substrate with a transparency of 80–90%.

#### Acknowledgements

We are grateful to Dr. D. Hines for guidance in transfer printing of carbon nanotubes and HMDS coating, Neetal Jagadeesh for assistance with calibration of the airbrush used, and Dr. V. Ballorotto for guidance on the spray coating of carbon nanotubes. This work has been supported by the Laboratory for Physical Sciences, and the UMD-MRSEC Shared Equipment Facilities, with infrastructure support from CNAM and the UMD NanoCenter.

#### References

- [1] H. Sirringhaus, *Adv. Mater.* 17 (2005) 2411.
- [2] S.R. Forrest, *Nature* 428 (2004) 911.
- [3] Y.G. Ha, E.A. You, B.J. Kim, et al., *Synth. Met.* 153 (2005) 205.
- [4] D.H. Zhang, K. Ryu, X.L. Liu, et al., *Nano Lett.* 6 (2006) 1880.
- [5] E. Cantatore, T.C.T. Geuns, G.H. Gelinck, et al., *IEEE J. Solid-State Circuits* 42 (2007) 84.
- [6] M.C. Hamilton, J. Kanicki, *IEEE J. Sel. Top. Quantum Electron.* 10 (2004) 840.
- [7] Lagemaat Jao van de, M. Barnes Teresa, Rumbles Garry, et al., *Appl. Phys. Lett.* 88 (2006) 233503.
- [8] A. Bachtold, M.S. Fuhrer, S. Plyasunov, et al., *Phys. Rev. Lett.* 84 (2000) 6082.
- [9] G. Gruner, *J. Mater. Chem.* 16 (2006) 3533.
- [10] Z.C. Wu, Z.H. Chen, X. Du, et al., *Science* 305 (2004) 1273; J.M. Bonard, T. Stora, J.P. Salvetat, et al., *Adv. Mater.* 9 (1997) 827.
- [11] M. Kaempgen, G.S. Duesberg, S. Roth, *Appl. Surf. Sci.* 252 (2005) 425; J.H. Lehman, C. Engtrakul, T. Gennett, et al., *Appl. Opt.* 44 (2005) 483; H.Z. Geng, D.S. Lee, K.K. Kim, et al., *J. Korean Phys. Soc.* 53 (2008) 979.
- [12] Y.I. Song, C.M. Yang, D.Y. Kim, et al., *J. Colloid Interface Sci.* 318 (2008) 365.
- [13] H.Z. Geng, K.K. Kim, K. Lee, et al., *NANO* 2 (2007) 157; S. Paul, D.W. Kim, *Carbon* (2009).
- [14] M. Jung de Andrade, M. Dias Lima, V. Skakalova, et al., *Phys. Status Solidi (RRL) – Rapid Res. Lett.* 1 (2007).
- [15] S.F. Pei, J.H. Du, Y. Zeng, et al., *Nanotechnology* 20 (2009).
- [16] P. Fournet, D.F. O'Brien, J.N. Coleman, et al., *Synth. Met.* 121 (2001) 1683; S.P. Lee, H. Choi, K.W. Lee, et al., *J. Korean Phys. Soc.* 48 (2006) 146.
- [17] S. Chaudhary, H.W. Lu, A.M. Muller, et al., *Nano Lett.* 7 (2007) 1973; M.A. Contreras, T. Barnes, J. van de Lagemaat, et al., *J. Phys. Chem. C* 111 (2007) 14045.
- [18] Chia-Hao Chang, Chao-Hsin Chien, Jung-Yen Yang, *Appl. Phys. Lett.* 91 (2007) 083502.
- [19] Y.Y. Zhang, Y.M. Shi, F.M. Chen, et al., *Appl. Phys. Lett.* 91 (2007) 223512.
- [20] C.H. Chang, C.H. Chien, J.Y. Yang, *Appl. Phys. Lett.* 91 (2007).
- [21] J.F. Chang, B.Q. Sun, D.W. Breiby, et al., *Chem. Mater.* 16 (2004) 4772.
- [22] Y. Xu, J.S. Gao, X.M. Zheng, et al., *J. Lumin.* 122 (2007) 908.
- [23] L. Hu, D.S. Hecht, G. Gruner, *Nano Lett.* 4 (2004) 2513.
- [24] A. Benor, A. Hoppe, V. Wagner, et al., *Org. Electron.* 8 (2007) 749.
- [25] B.H. Hamadani, D. Natelson, *Appl. Phys. Lett.* 84 (2004) 443.
- [26] Vanoni Claudio, Tsujino Soichiro, A. Jung Thomas, *Appl. Phys. Lett.* 90 (2007) 193119; Kumaki Daisuke, Umeda Tokiyoshi, Tokito Shizuo, *Appl. Phys. Lett.* 92 (2008) 013301.
- [27] V. Pesavento Paul, P. Puntambekar Kanan, C. Daniel Frisbie, et al., *J. Appl. Phys.* 99 (2006) 094504.
- [28] B.H. Hamadani, D. Natelson, *J. Appl. Phys.* 95 (2004) 1227.
- [29] N. Koch, A. Kahn, J. Ghijsen, et al., *Appl. Phys. Lett.* 82 (2003) 70; P.V. Necliudov, M.S. Shur, D.J. Gundlach, et al., *J. Appl. Phys.* 88 (2000) 6594; D. Kumaki, T. Umeda, S. Tokito, *Appl. Phys. Lett.* 92 (2008).

- [30] P. Puntambekar Kanan, V. Pesavento Paul, C. Daniel Frisbie, *Appl. Phys. Lett.* **83** (2003) 5539.
- [31] P.F. Qi, A. Javey, M. Rolandi, et al., *J. Am. Chem. Soc.* **126** (2004) 11774.
- [32] L. Burgi, T.J. Richards, R.H. Friend, et al., *J. Appl. Phys.* **94** (2003) 6129.
- [33] Cao Qing, Zhu Zheng-Tao, G. Lemaitre Maxime, et al., *Appl. Phys. Lett.* **88** (2006) 113511.
- [34] D.R. Hines, V.W. Ballarotto, E.D. Williams, et al., *J. Appl. Phys.* **101** (2007) 024503.